EUROPEAN ORGANIZATION FOR NUCLEAR RESEARCH
European Laboratory for Particle Physics

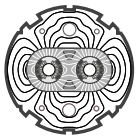

Large Hadron Collider Project

LHC Project Report 367

A beam separation and collision scheme for IP2 and IP8 at the LHC for optics version 6.1

O. Brüning and W. Herr, SL Division,
R. Ostojic, LHC Division, CERN, 1211-Geneva 23

Abstract

In this report we describe the proposed beam separation and collision schemes for interaction points 2 (ALICE experiment) and 8 (LHCb) in the LHC for optics version 6. The original proposal for optics version 5 was redesigned to be compatible with new requirements and the existing hardware. Contrary to the original scheme, in our scenario some magnets in the common part of the two rings are used to establish part of the separation. However, individual control of the two beams remains fully possible. The necessary corrector strengths are significantly smaller and the aperture requirements less severe. Furthermore, this new scheme would allow to further increase the crossing angle, if required. To achieve this, the compensation scheme of the spectrometer magnets in IP2 and IP8 had to be redesigned and the implication of the desired alignment of these magnets was studied.

Administrative Secretariat
LHC Division
CERN
CH-1211 Geneva 23
Switzerland

Geneva, 17 January 2000

1 Introduction

The CERN Large Hadron Collider (LHC) is designed for highest luminosity and therefore requires an operation with a large number of bunches [1]. The bunches are closely spaced (25 ns) and in order to avoid unwanted collisions in the part where the two beams share a common vacuum chamber, the beams must collide at a small crossing angle in all experimental interaction regions [2]. The basic issues of a beam separation scheme are described in an earlier report [3] where the scenario for interaction regions 1 (ATLAS) and 5 (CMS) are described. The ALICE experiment in IP2 is designed for experiments with ions but should allow data taking at a reduced interaction rate with proton beams. This leads to a large range of boundary conditions for the optics in IP2 [4]. Furthermore, the injection system for ring 1 of the LHC is located close to the ALICE experiment and imposes further constraints. The LHCb experiment in IP8 aims at average luminosities between 1 - 5 $\cdot$ 10^{32} cm^{-2}s^{-1}. To compensate for a loss of luminosity at lower bunch intensities, the required β^* at the interaction point ranges from 1.0 to 50 meters. The interaction region 8 also houses the injection equipment for ring 2. The crossing and compensation scheme has to allow for this required flexibility. In the original crossing and separation scheme it was foreseen to cross vertically in both experiments.

1.1 Optics and modes of operation for IP2

The operation with ions differs significantly from the proton operation. The bunch spacing is 125 ns (25 ns for protons) and the bunch intensities are some orders of magnitude smaller than for proton bunches. The required optics parameters and bunch intensities are summarized in [4]. The β-function at the interaction point can vary from 0.5 m to 50 m for ion operation and for proton operation $\beta^* = 10$ m is foreseen. Since this would still give too high interaction rates, the two proton beams do not collide head on but with a finite separation, adjusted to fit the specifications [4]. A separation and collision scheme must therefore allow for a large range of collision optics as well as for the option to collide with a transverse offset of several times the transverse beam size. The larger bunch spacing and lower bunch intensity for ion operation reduces the separation requirements since the number of long range collisions [2] and their detrimental effects are significantly smaller.

1.2 Optics and modes of operation for IP8

The main difference compared to other experiments is the shifted interaction point. In order to accommodate the single arm spectrometer in the existing hall, the interaction point and the focussing quadrupoles are displaced by $3\lambda_{RF}/2$ (≈ 11.22 m) towards IP7. The implications of this shift on the beam dynamics, in particular on beam-beam effects are discussed in [8]. At collision it is desired to adjust the optics to fulfill the luminosity requirements dynamically, i.e. to keep the luminosity approximately constant during one run or for different beam intensities.

2 Spectrometer dipole magnet compensation

The experiments in IP2 and IP8 both use spectrometer magnets which distort the beam trajectories in the vicinity of the interaction point and around the machine and their effect has to be compensated locally with dedicated compensation magnets. Since these strongly interfere with the crossing and separation scheme, the design of the compensation scheme is important and requires attention. These compensators are all placed in the straight sections between the interaction point and the final focussing triplet.

2.1 Spectrometer magnet compensation in ALICE

The experiment uses a spectrometer magnet inside the muon detector. It is positioned at about 10 m from the IP towards IP3, is 3 m long and the integrated field is 3.2 Tm in the horizontal direction. In the original design this magnet is off during injection and ramping and is compensated with 2 compensator magnets of the types MCBWA, positioned at a distance of 20 m on both sides of IP2. The compensator magnets fully

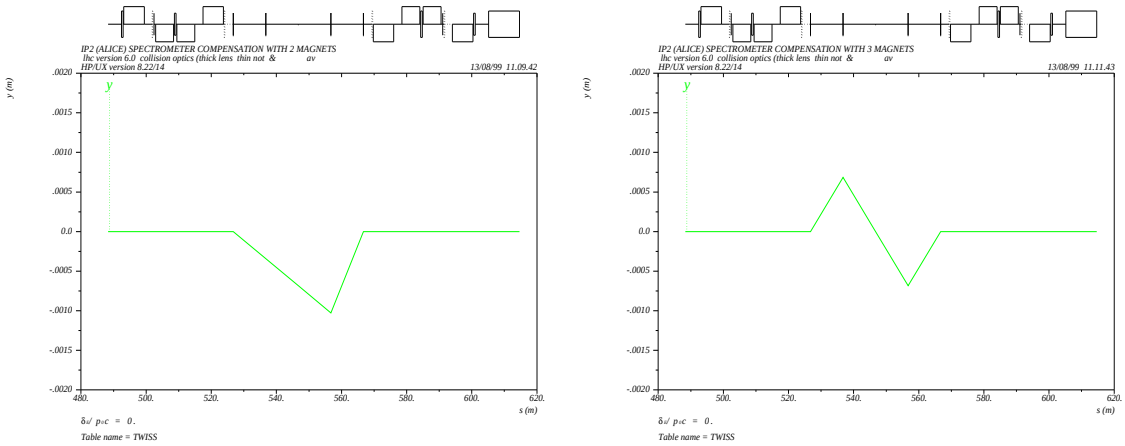

Figure 1: ALICE spectrometer magnet compensated with 2 (left) or 3 (right) compensation magnets. Interaction point is at the centre.

compensate the effects outside the bump, but create a vertical angle and vertical offset at the interaction point.

Without additional compensation, this bump (see Fig. 1, left) produces a vertical offset of ≈ 0.7 mm and an angle of ≈ 35 μrad. Since all magnets are common to both beams, they generate a separation of 1.4 mm and a full crossing angle of ≈ 70 μrad. Furthermore, the experiment may require a polarity reversal of the magnet, producing angles and offsets of opposite sign. Both, the angle and the offset must be taken into account and compensated with the separation and crossing scheme. In particular the compensation of the vertical offset requires very large correction strengths [4, 5]. Furthermore, such a non-local correction is sensitive to errors or changes to the optics in the interaction region and would not allow to easily change the β-function at the collision point. A possible solution is to add a third compensation magnet, preferably symmetric to the spectrometer magnet on the other side of the interaction point. This adds one degree of freedom for the correction and the offset at the interaction point can be corrected to zero producing an antisymmetric bump. The vertical angle (α_{spec}) is still present and twice as large, i.e. $\approx \pm 70$ μrad, producing a full crossing angle of $\alpha \approx \pm 140$ μrad but the vertical offset is automatically compensated all the time and for all modes of operation and therefore needs no special attention (see Fig. 1, right). Moreover, the spectrometer compensation bump is completely decoupled from optics and orbit manipulations and therefore highly desirable for the operation. The necessary parameters for the proposed full compensation scheme are given in Table 1.

2.2 Spectrometer magnet compensation in LHCb

The LHCb experiment uses a spectrometer magnet which is positioned approximately 5.0 m from the IP towards IP1, it is 1.92 m long and the integrated field at 7 TeV

Magnet	type	length (m)	distance from IP (m)	$\int Bdl$ (Tm)
Compensator 1	MCBW	1.7	-20.066	1.555
Spectrometer		3.0	-9.75	3.200
Compensator 2	MBXW	3.4	9.75	3.200
Compensator 3	MCBW	1.7	20.066	1.555

Table 1: *Proposed spectrometer compensation for ALICE with three compensator magnets.*

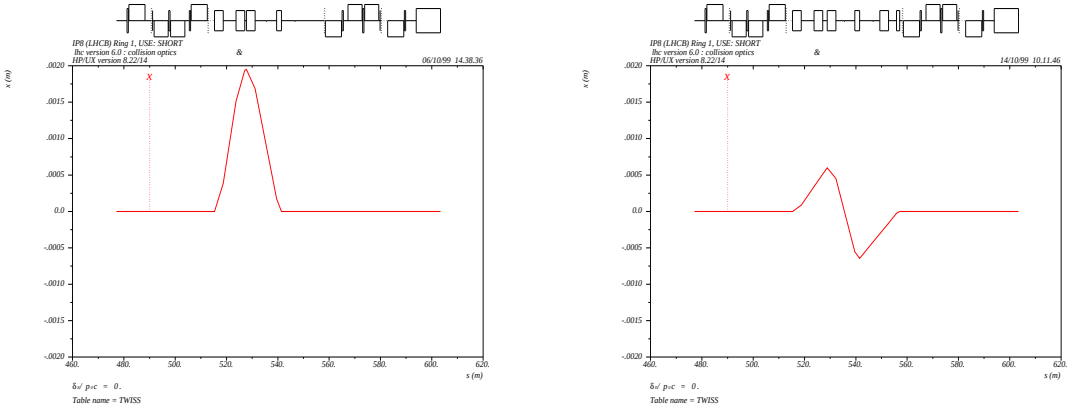

Figure 2: LHCb spectrometer magnet compensated with 2 (left) or 3 (right) compensation magnets. Interaction point is at the centre.

is 4.2 Tm in the vertical direction. In previous schemes this spectrometer magnet was compensated with 2 independent magnets only, producing a horizontal offset and angle at the interaction point. The magnet is warm and is ramped proportional to the beam energy and therefore these distortions are the same at injection and at top energy. Without additional compensation, this bump (see Fig. 2, left) produces a horizontal offset of $\approx$ 0.9 mm and an angle of $\approx$ 180 μrad and therefore a separation of 1.8 mm and a crossing angle of $\approx$ 360 μrad. Furthermore, the experiment requires a polarity reversal of the magnet, producing angles and offset of opposite sign. As already observed for IP2, the compensation of the horizontal offset requires too large correction strength [6] if it is achieved with correctors near insertion quadrupoles. The preferred solution is again the addition of a third compensation magnet beyond the spectrometer magnet on the same side. The offset at the interaction point is now always compensated and with the full field of the spectrometer, the angle α_{spec} produced is $\pm$ 135 μrad in the horizontal plane. The spectrometer bump is completely decoupled from optics and orbit manipulations and allows to change the optics if required. In particular it allows to change the β^* at the interaction point without separating the beams. The parameters for the proposed compensation scheme are given in Table 2. The mechanical layout for the spectrometer dipole compensation in IP2 and IP8 is shown in Fig. 23 in Appendix A.

Magnet	Type	length (m)	distance from IP (m)	$\int Bdl$ (Tm)
Compensator 1	MCBWB	1.00	20.416	1.08
Spectrometer		1.92	5.25	4.20
Compensator 2	MBXW	3.40	-5.25	4.22
Compensator 3	MCBW	1.70	-20.066	1.10

Table 2: *Proposed spectrometer compensation for LHCb with three compensator magnets at top energy (7 TeV).*

3 Crossing and separation scheme

In collision, the separation of the unwanted encounters is provided by the finite crossing angle. For adjustment of the collision, it is required to have individual control of the two beams, at least over a large range of the crossing angle and collision offset [3]. The collision optics with $\beta^* = 10$ m is also used for injection for both, IP2 and IP8 and the separation scheme is therefore valid for collision at $\beta^* = 10$ m and injection, although the aperture requirements are tighter at injection.

3.1 Separation requirements

The basic parameters taking into account the above boundary conditions are summarized in Tables 3 (IP2) and 4 (IP8) for the main phases of operation, i.e. injection, ramp, pre-collision and collision. The minimum separation should not become smaller than 10 σ at any of the parasitic encounters. The parallel separation refers to the separation of the central head-on collision point. In the presence of a separation in both planes, the minimum separation d_{min} is calculated from the total distance of the beams using the largest transverse beam size for the normalization. The studies [9] also indicate that it could be necessary to further increase the crossing angle for very high beam intensities.

3.2 Separation strategies

The possible strategies to establish a sufficient crossing angle while keeping individual control of the two beams were described in detail in [3]. However, the rather large range of optics configuration may require different strategies for the various options, although the higher β^* configurations should make it easier to obtain the required separation. For the design of a crossing angle in IP2 and IP8, there is a very significant difference to the low β interaction regions IP1 and IP5. While for the latter the phase advance between the interaction point and the first dedicated correctors near Q4 is close to $\pi/2$, this phase advance is close to π for IP2 and IP8. This is ideal to produce an angle with minimal strength of the used correctors. It is therefore not necessary or advantageous to use common corrector magnets for the crossing angle like they were used for IP1 and IP5 [3]. However they are very useful to produce a parallel bump. For the smaller β^* they become important to reduce the required strengths on the other corrector magnets. The maximum strengths of the available corrector magnets and their properties are given in Table 5 in the appendix. It is unavoidable to use closed orbit correctors for a fine adjustment of the bumps, but in order not to reduce the correction capabilities, the strengths used for the separation scheme never exceed 20% of their maximum.

State	SPEC	$\beta^*_{x,y}$ (m)	half external angle α_{ext} (μrad)	half crossing angle α (μrad)	parallel separation (mm)	d_{ip} (σ)	d_{min} (σ)
Injection	OFF	10.0	$\pm$ 210.0*	$\pm$ 210.0	$\pm$ 2.00	14.3	10.8
End of ramp	OFF	10.0	$\pm$ 100.0	$\pm$ 100.0	$\pm$ 0.80	22.6	22.6
Pre-collision	neg	0.5	$\pm$ 170.0*	$\pm$ 100.0	$\pm$ 0.10	12.6	6.4
Collision	neg	0.5	$\pm$ 170.0*	$\pm$ 100.0	0.0	-	6.3
Pre-collision	pos	0.5	$\pm$ 80.0	$\pm$ 150.0	$\pm$ 0.10	12.6	3.7
Collision	pos	0.5	$\pm$ 80.0	$\pm$ 150.0	0.0	-	3.6
Pre-collision	neg	10.0	$\pm$ 170.0	$\pm$ 100.0	$\pm$ 0.80	22.6	22.6
Collision	neg	10.0	$\pm$ 170.0	$\pm$ 100.0	0.0	-	10.0
Pre-collision	pos	10.0	$\pm$ 80.0	$\pm$ 150.0	$\pm$ 0.80	22.6	17.3
Collision	pos	10.0	$\pm$ 80.0	$\pm$ 150.0	0.0	-	14.9
Pre-collision	neg	50.0	$\pm$ 105.0*	$\pm$ 35.0	$\pm$ 0.50	6.3	6.3
Collision	neg	50.0	$\pm$ 105.0*	$\pm$ 35.0	0.0	-	4.3
Pre-collision	pos	50.0	$\pm$ 80.0	$\pm$ 150.0	$\pm$ 0.50	6.3	6.3
Collision	pos	50.0	$\pm$ 80.0	$\pm$ 150.0	0.0	-	18.5

* maximum possible due to strength or aperture

Table 3: *Proposed separation conditions in IP2. The angles shown are the external angle α_{ext} and the final crossing angle $\alpha = \alpha_{ext} + \alpha_{spec}$. The corresponding separation in units of the beam size are given for the interaction point (d_{ip}) and the minimum (d_{min}) in the whole common part, always using the largest beam size for the normalization and assuming a normalized emittance of 3.75 μm. Operation at $\beta^* = 0.5$ m and 50 m is planned for ions only and therefore does not require a large separation in the drift space.*

3.3 Crossing angle in IP2

A complication for the vertical crossing angle in IP2 is the vertical angle already produced by the horizontal field of the spectrometer magnet and its compensators. Furthermore, it is desired to allow both polarities of the spectrometer magnet. As it was already discussed, the spectrometer compensation bump already produces a crossing angle (α_{spec}) and local separation. This bump is not long enough to separate the beams sufficiently at all parasitic encounters, but it can be used as an integral part of the crossing scheme. However, the mechanical aperture of the injection septum and kicker impose constraints for the beam optics and separation at injection. Satisfying the aperture requirements at the exit of the kicker required a vertical orbit of 2.7 mm [6, 7] for previous versions of the optics. Although there are indications that this offset is not required with the new separation scheme and the new optics, we allow for such a request in case of problems. Such an orbit offset would fix the sign of the crossing angle [4] and therefore the crossing scheme must be flexible enough to allow both polarities with the same sign of the angle, should this become necessary. In the case the angle produced by the spectrometer α_{spec} has not the same sign as the desired angle α (*neg* in Table 3), the necessary angle from the separation scheme α_{ext} must be larger by that amount, requiring a larger

State	$\beta^*_{x,y}$ (m)	half external angle α_{ext} (μrad)	half crossing angle α (μrad)	parallel separation (mm)	d_{ip} (σ)	d_{min} (σ)
Injection	10.0	$\pm$ 210.0*	$\pm$ 245.0	$\pm$ 2.00	14.3	10.8
End of ramp	10.0	$\pm$ 100.0	$\pm$ 235.0	$\pm$ 0.50	14.1	14.1
Pre-collision	10.0	$\pm$ 100.0	$\pm$ 235.0	$\pm$ 0.50	14.1	14.1
Collision	10.0	$\pm$ 100.0	$\pm$ 235.0	0.0	-	18.0
Collision	10.0	$\pm$ 65.0	$\pm$ 200.0	0.0	-	12.0
Pre-collision	1.0	$\pm$ 150.0	$\pm$ 285.0	$\pm$ 0.25	22	10.0
Collision	1.0	$\pm$ 150.0	$\pm$ 285.0	0.0	-	10.0
Pre-collision	50.0	$\pm$ 105.0*	$\pm$ 240.0	$\pm$ 1.00	12.6	12.6
Collision	50.0	$\pm$ 105.0*	$\pm$ 240.0	0.0	-	11.4

* maximum possible due to strength or aperture

Table 4: *Proposed separation conditions in IP8. The shown angles are the external angle α_{ext} and the final crossing angle α.*

aperture and increased strength of the correctors, producing large separation outside the spectrometer bump. Such a crossing angle bump is shown in Fig. 3 and the corresponding strengths are given in Table 6. The required strengths are still well below the possible maximum. In the case the two crossing angles have the same sign (*pos* in Table 3), the actual angle at the crossing point is larger because one has to provide sufficient separation outside the spectrometer bump. However, the necessary strengths and the required aperture are still significantly smaller than for the other polarity as shown in Fig. 4 and Table 7. For ion operation a smaller β^* is foreseen. The crossing angle bumps for both polarities of the spectrometer dipole and $\beta^* = 0.5$ m are shown in Figs. 5 and 6. The corresponding strengths are given in Tables 8 and 9.

Since only operation with ions is foreseen with $\beta^* = 0.5$ m, the required minimum separation is smaller since the intensity is lower and the bunch distance much larger, leading to strongly reduced long range beam-beam effects. The Fig. 7 shows the required aperture for the largest bump amplitude. The aperture requirements for the separation bumps have to be calculated taking into account the available aperture, the actual optics, beam parameters and possible orbit errors. The aperture is quoted in terms of n_1, the maximum allowed position of the primary collimator in units of the beam size which provides sufficient protection of the magnets. This value should not become smaller than ≈ 7 in Fig. 7. The values n_1 are calculated with the aperture program apl [11], using a peak closed orbit distortion of 4 mm, a momentum error of 0.1%, a β-beating of 20% and standard mechanical tolerances [11]. At injection, the required crossing angle is $\pm$ 210 μrad (Table 3). The resulting crossing angle bump is shown in Fig. 8 and the corresponding strengths in Table 10. The required aperture at injection energy for the $\beta^* = 10$ m optics is shown in Fig. 9. In all cases the aperture is sufficient using the criteria defined above. As mentioned above, the injection into ring 1 in interaction region 2 imposes constraints for the optics and separation [7]. The aperture constraints at the kicker MKI could require

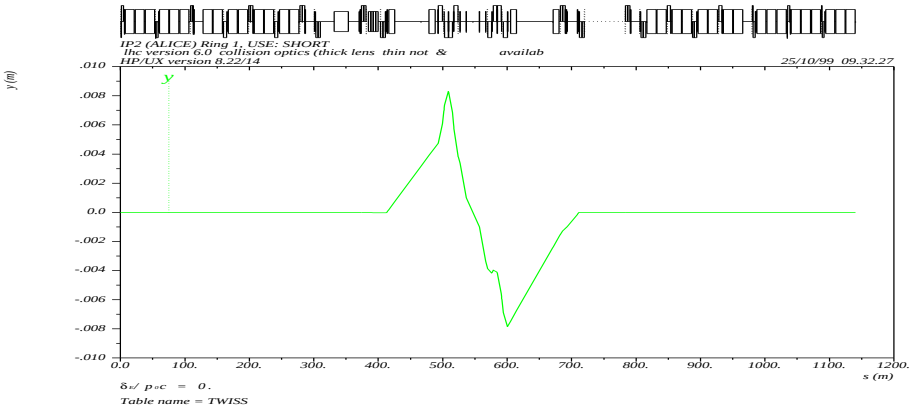

Figure 3: Vertical crossing angle in IP2, $\beta^* = 10$ m, $\alpha = \pm\ 100$ μrad, spectrometer magnet negative, compensated with 3 compensators, Table 6.

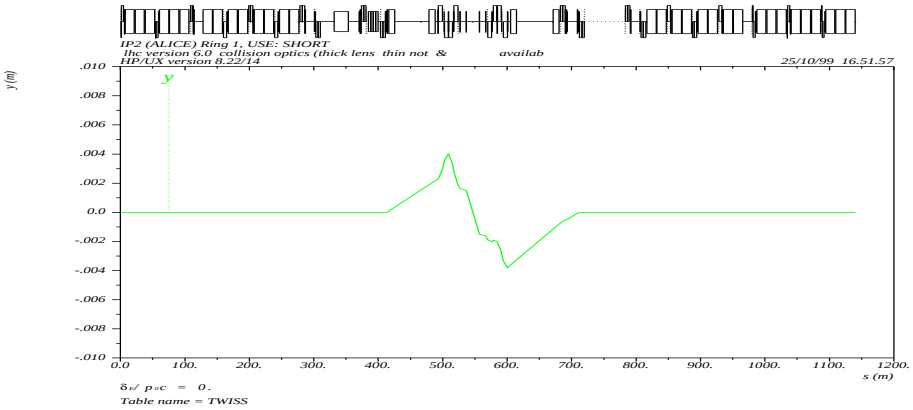

Figure 4: Vertical crossing angle in IP2, $\beta^* = 10$ m, $\alpha = \pm\ 150$ μrad, spectrometer magnet positive, compensated with 3 compensators, Table 7.

a vertical orbit up to 2.7 mm at the MKI for ring 1 [6, 7]. This must be superimposed onto the separation bump for ring 1 only. Such a bump superimposed is shown in Fig. 10. This scheme requires an additional corrector magnet between the septum and the Q5 doublet. The required strengths for the added bump are given in Table 11. The additional corrector is also very useful to control the orbit and angle of the beam in the injection region. In case this bump is not necessary, the sign of the crossing angle can be chosen freely to match the spectrometer polarity (labelled *pos* in Table 3).

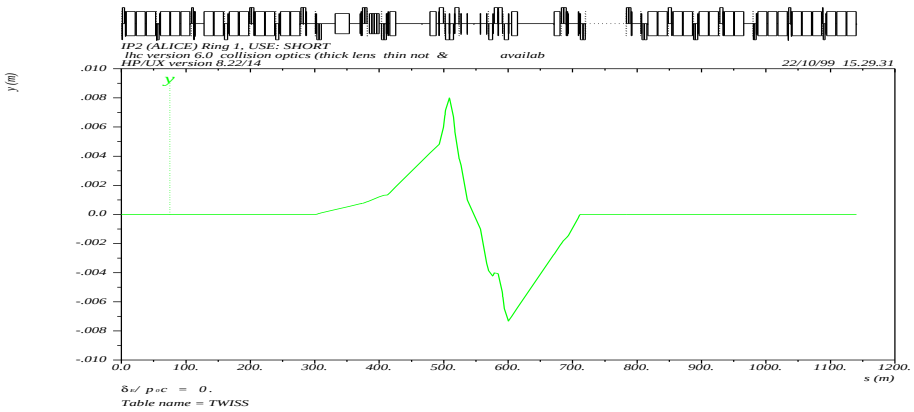

Figure 5: Vertical crossing angle in IP2, $\alpha = \pm$ 100 μrad, spectrometer magnet negative, compensated with 3 compensators, for $\beta^* = 0.5$ m, Table 8.

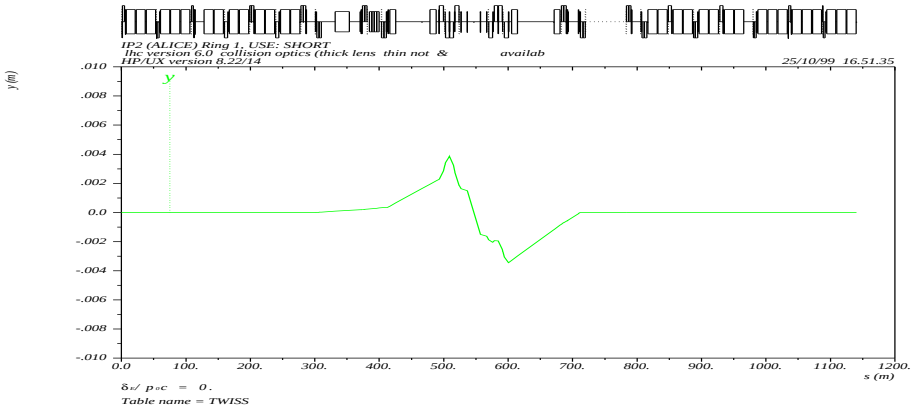

Figure 6: Vertical crossing angle in IP2, $\alpha = \pm$ 150 μrad, spectrometer magnet positive, compensated with 3 compensators, for $\beta^* = 0.5$ m, Table 9.

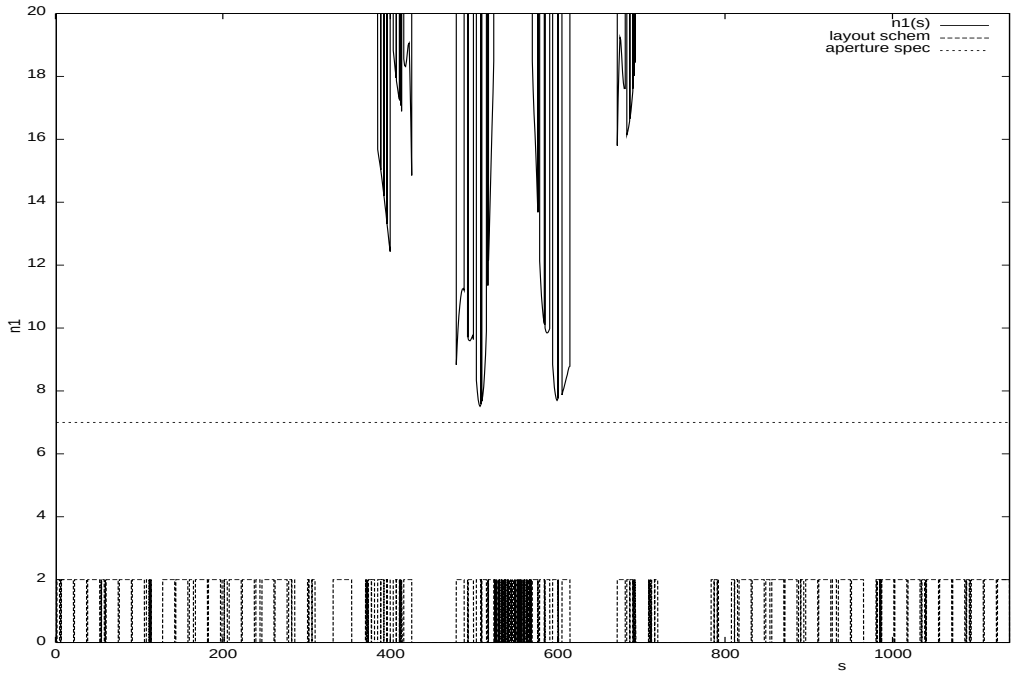

Figure 7: Required aperture in IP2, spectrometer magnet negative for ± 100 μrad and $\beta^* = 0.5$ m at collision energy.

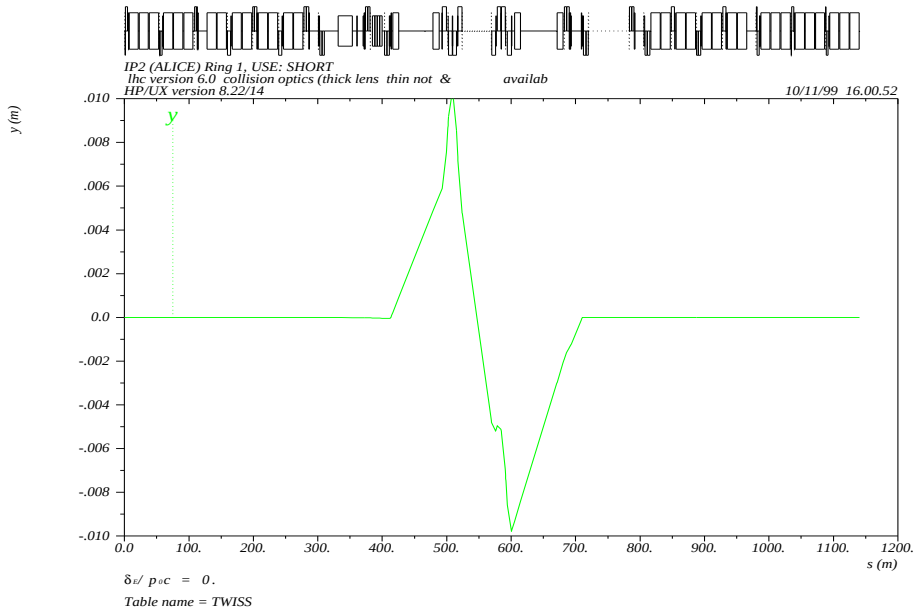

Figure 8: Crossing angle at injection in IP2, spectrometer magnet off, for ± 210 μrad and $\beta^* = 10$ m.

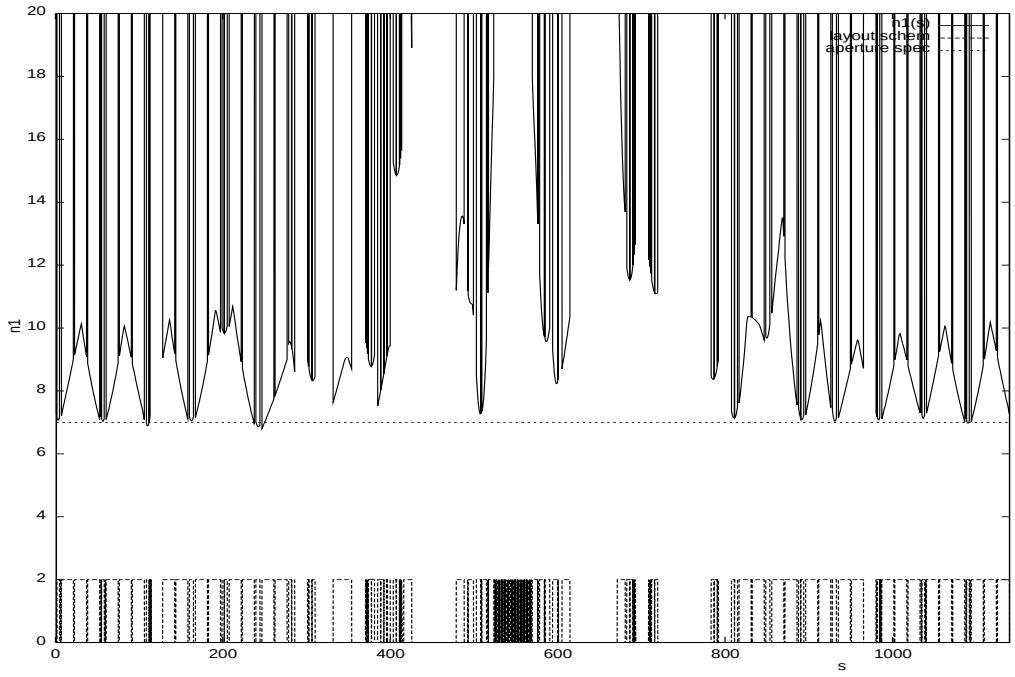

Figure 9: Required aperture in IP2, spectrometer magnet off, for $\pm$ 210 μrad and $\beta^* = 10$ m at injection energy.

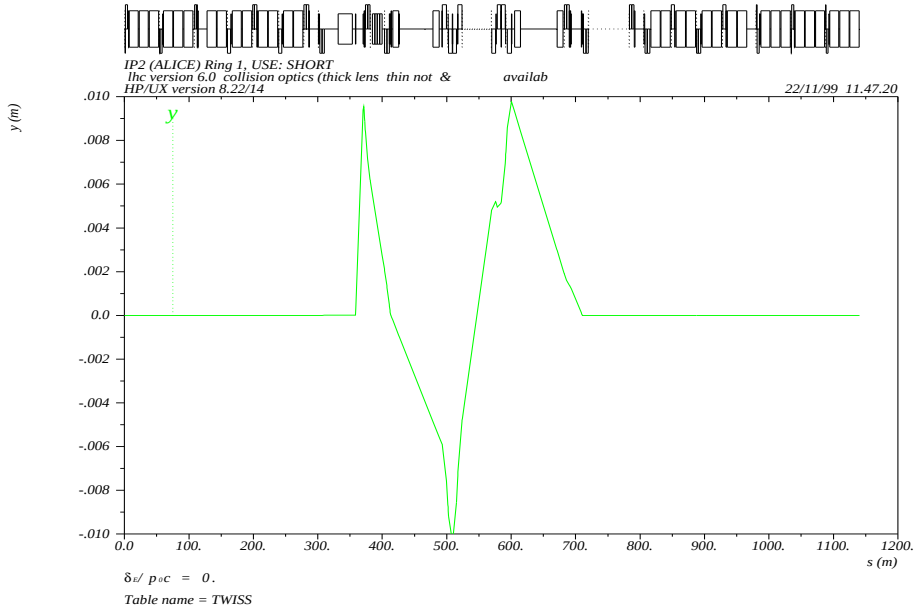

Figure 10: Crossing angle at injection in IP2, spectrometer magnet off, for $\pm$ 210 μrad and $\beta^* = 10$ m. As Fig. 8, but with offset of 2.7 mm at exit injection kicker.

3.4 Crossing angle in IP8

Two important features of the LHCb spectrometer have suggested to reconsider the crossing scheme in IP8: first the spectrometer magnet is warm and can be ramped [10], and secondly, it produces a rather large, unavoidable crossing angle in the horizontal plane of $\alpha_{spec} = \pm$ 135 μrad at all energies. It was therefore suggested to design the

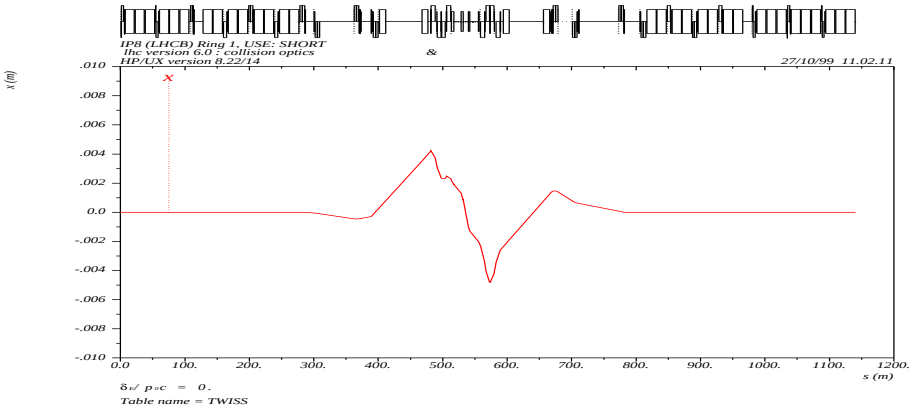

Figure 11: Horizontal crossing angle $\alpha_{ext} = \pm$ 100 μrad in IP8, spectrometer magnet on, compensated with 3 compensators, for β^* =10 m, Table 12.

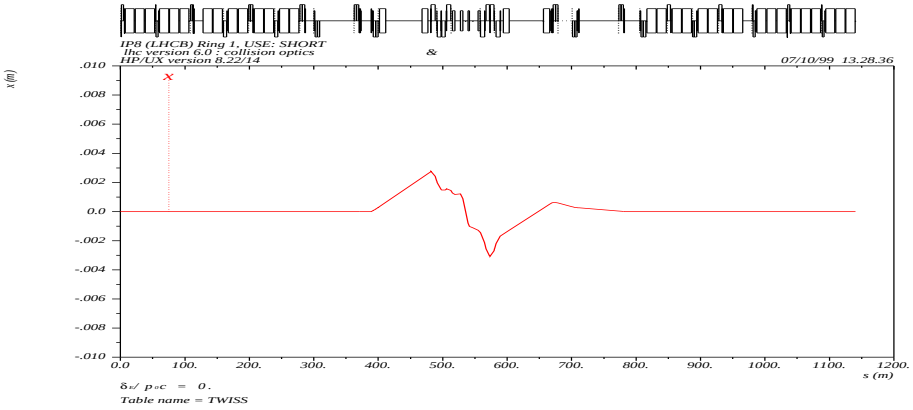

Figure 12: Horizontal crossing angle $\alpha_{ext} = \pm$ 65 μrad in IP8, spectrometer magnet on, compensated with 3 compensators, for β^* =10 m.

crossing scheme in the horizontal plane to avoid possible operational difficulties that may be associated with a crossing in two planes simultaneously. An interference with the injection scheme is automatically avoided and the sign of the crossing angle bump can be chosen to match the angle produced by the spectrometer compensation bump. The external bumps can therefore be designed independent of the spectrometer polarity because for both polarities they are then identical but with opposite sign. However, one of the two polarities may be more desirable: the crossing angle bump as well as the beam separation dogleg provided by the D1 and D2 magnets create some residual horizontal dispersion. It is advantageous to run with the sign of the bump where the dispersion at least partially compensates rather than adds together. This is the case for a bump

with the field of the spectrometer downwards and corresponds to the crossing bumps shown in Figs. 11,12 and 13. Unfortunately, the separation produced by the spectrometer bump alone is not sufficient because it is too short to separate the beams at all unwanted collisions and an additional crossing angle bump is superimposed. This is shown in Fig. 11 where an external crossing angle designed for $\alpha_{ext} = \pm$ 100 μrad is superimposed on the spectrometer bump, thus producing a steepening and rather large crossing angle at the interaction point of approximately $\alpha = \pm$ 235 μrad. The corresponding strengths are given in Table 12. The resulting separation is however larger than required and in Fig. 12 a design angle of $\alpha_{ext} = \pm$ 65 μrad was superimposed, producing a minimum normalized separation of at least 12 σ everywhere, which is considered sufficient. The aperture and strength requirements are significantly reduced and the actual crossing angle at the collision point is exactly $\alpha = \pm$ 200 μrad.

To compensate for lower intensities, smaller β^* are foreseen: the crossing angle bump for $\beta^* = 1$ m is shown in Fig. 13 and the strengths are given in Table 13. The Fig. 14

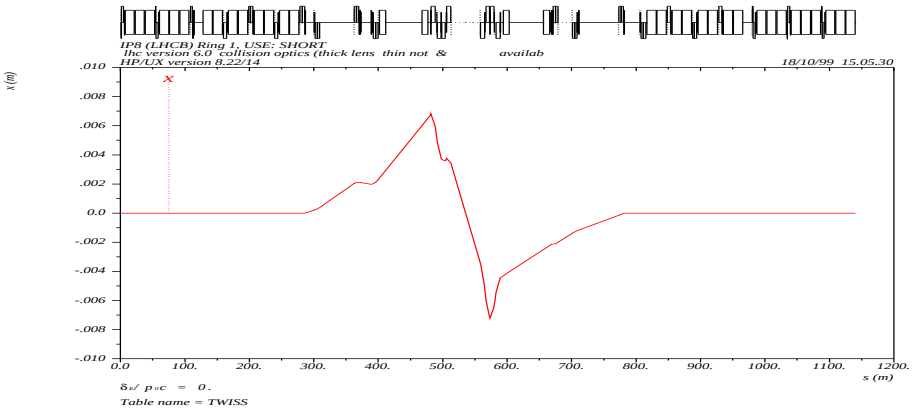

Figure 13: Horizontal crossing angle $\alpha_{ext} = \pm$ 150 μrad in IP8, for $\beta^* = 1.0$ m.

shows the required aperture for the crossing angle of $\alpha_{ext} = \pm$ 150 μrad and $\beta^* = 1.0$ m. The required aperture at injection is very similar to the case of IP2 as presented in Fig. 9. As it can be seen from Table 4, the crossing angle in IP8 cannot be larger than $\pm$ 105 μrad for $\beta^* = 50.0$ m due to strength limitations.

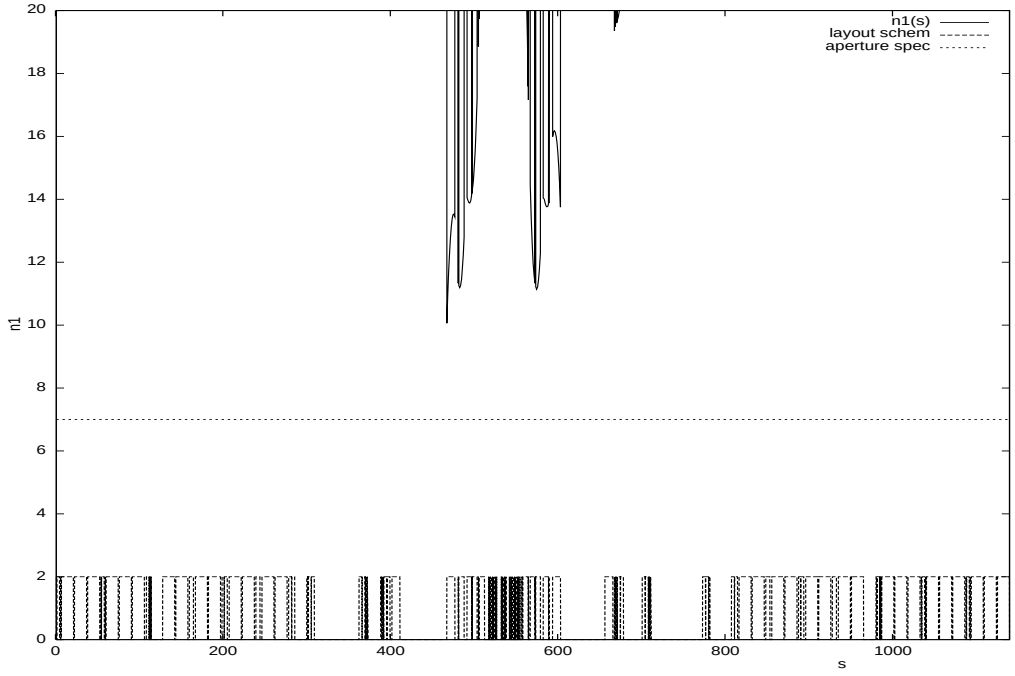

Figure 14: Required aperture in IP8, for $\alpha_{ext} = \pm$ 150 μrad and $\beta^* = 1.0$ m.

3.5 Horizontal and vertical parallel separation

Both interaction regions need a parallel separation bump at injection, during the ramp, and before the collision. Moreover, such a parallel separation is required for the ALICE experiment to control the luminosity in proton operation. The strategy used for this separation is identical to that described in [3] for IP1 and IP5 and only the results are presented. A parallel horizontal bump of ± 1 mm in IP2 is shown in Fig. 15 for $\beta^* = 10$ m and the correctors used are shown in Table 14. For $\beta^* = 0.5$ m in IP2, the parallel horizontal bump is shown in Fig. 16 and the strengths are given in Table 15. Similar, a parallel vertical bump for IP8 is defined in Fig. 17 and Table 16. To demonstrate the

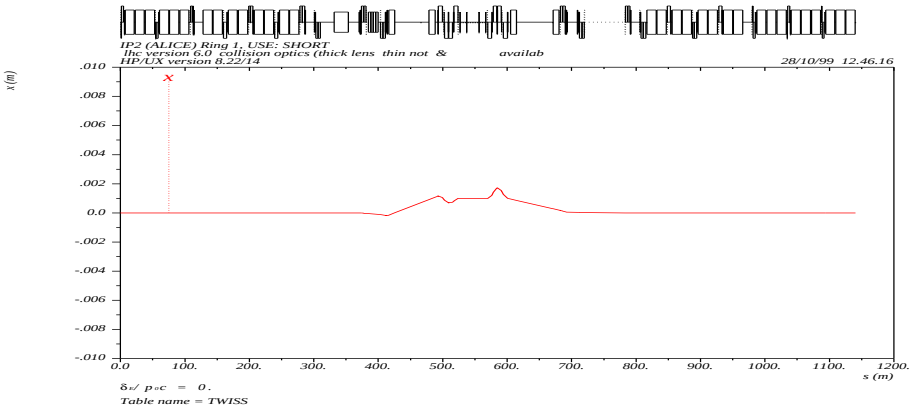

Figure 15: Horizontal bump 1 mm in IP2, for $\beta^* = 10$ m. Strengths in Table 14.

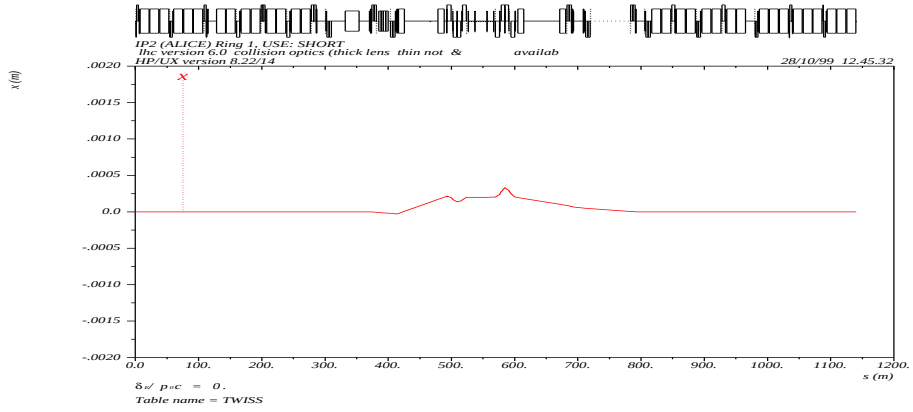

Figure 16: Horizontal bump 0.2 mm in IP2, for $\beta^* = 0.5$ m. Strengths in Table 15.

parallel separation for a smaller β^* in IP8, the parallel vertical bump for $\beta^* = 1$ m is shown in Fig. 18 and the strengths are given in Table 17.

4 Alignment of spectrometer magnet with respect to machine plane

The LHC tunnel is slightly tilted with respect to the horizontal plane. The average slope of the machine is 1.42% and the lowest point is close to IP8, i.e. LHCb. The machine elements are aligned in this plane, but it is desired to align the spectrometer magnets to the truly horizontal plane of the experimental halls. This introduces a small distortion

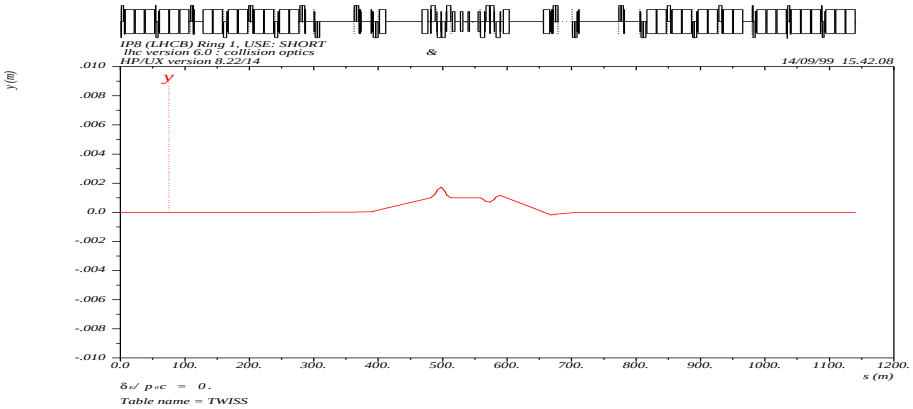

Figure 17: Vertical bump 1 mm in IP8, for $\beta^* = 10$ m. Strengths in Table 16.

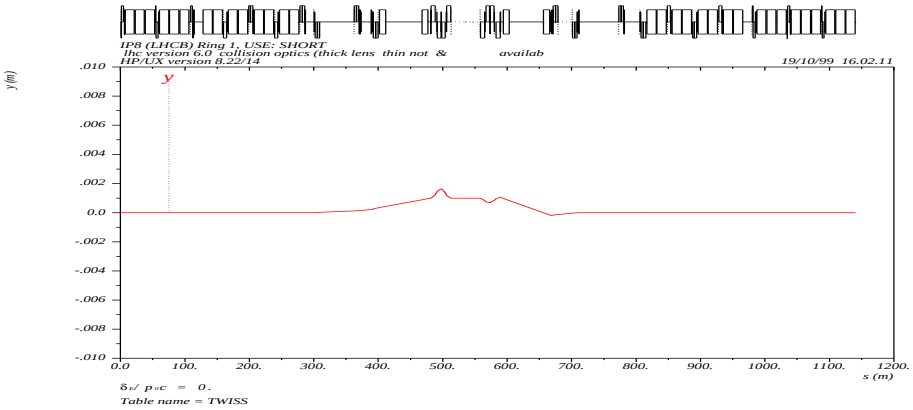

Figure 18: Vertical bump 1 mm in IP8, for $\beta^* = 1.0$ m. Strengths in Table 17.

of the beam trajectories. The main consequences of this different alignment are a small rotation of the field direction around the direction of the beam, creating a small transverse magnetic field, and a small slope with respect to the beam axis. In case of a vertical field, the latter creates a small field along the direction of the beam, but since this angle with respect to the beam is very small, its effect is negligible. The magnitude of the other effect, i.e. the rotation around the beam axis, depends on the position in the ring and is maximum where the ring is highest and lowest, i.e. near LHCb, where it is close to 1.4% or 11 mrad. The uncorrected effect of such a tilt is shown in Fig. 19. It creates a vertical offset at the collision point of 33 μm and therefore requires a correction. The compensator magnets can be used for this correction when they are *all* tilted by the same amount, producing a small, closed antisymmetric bump in the plane perpendicular to the field direction without an offset at the collision point and a small vertical angle of ≈ 1 μrad (Figs. 20). A similar picture can be obtained in IP2, although the effect is smaller since the spectrometer magnet is weaker and the tilt angle is smaller at the position of IP2 (see Fig. 21 and 22). This method of correction requires all compensators and spectrometers to be aligned in the same plane, thus producing automatically and always the necessary compensation of the tilt.

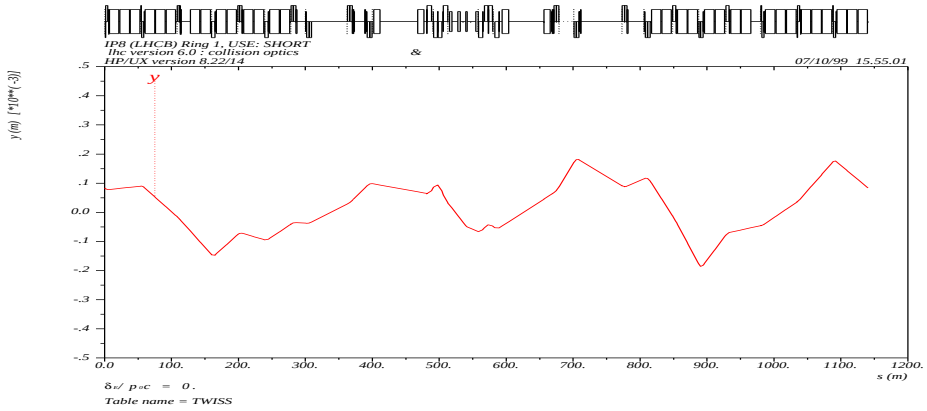

Figure 19: Spectrometer magnet tilted in IP8, not corrected.

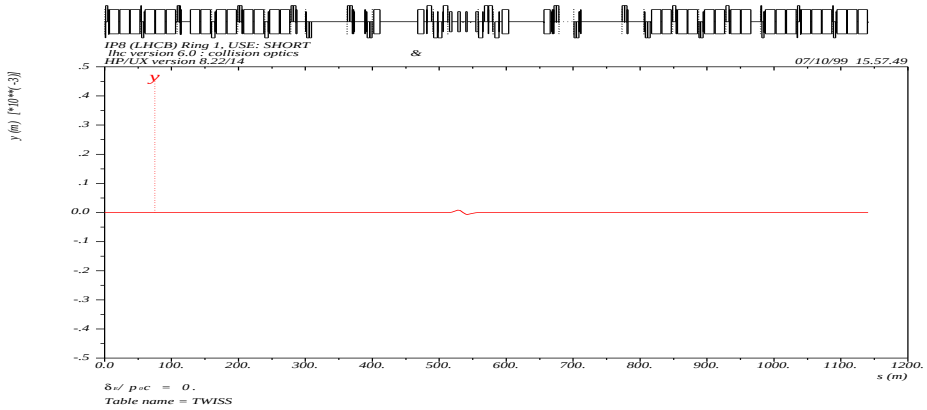

Figure 20: Spectrometer magnet tilted in IP8, corrected by tilting compensator magnets.

5 Summary

We present a proposal for a beam crossing and separation scheme for interaction points 2 and 8. It fulfills the requirements from beam dynamics and constraints imposed by the hardware. To achieve this, the redesign of the compensation schemes for the spectrometers in ALICE and LHCb was essential and allows a more flexible operation of the machine. In particular the collisions of the two beams can be ensured for all optics conditions in the insertions. The question of the relative alignment of the spectrometer magnets with respect to the machine was addressed as well and a solution proposed.

References

[1] LHC Conceptual Design, CERN/AC/95-05, (1995).

[2] W. Herr; *Beam-beam effects in the LHC*, Part. Acc. **50** (1995) 69.

[3] O. Brüning, W. Herr and R. Ostojic; *A beam separation and collision scheme for IP1 and IP5 at the LHC for optics version 6.0*, LHC Project Report 315 (1999).

[4] O. Brüning; *Optics Solutions in IR2 for Ring-1 and Ring-2 of the LHC Version 6.0*, LHC Project Note 188 (1998).

[5] J. Miles; *A Baseline Beam Separation Scheme for the LHC*, LHC Project Note 136 (1998).

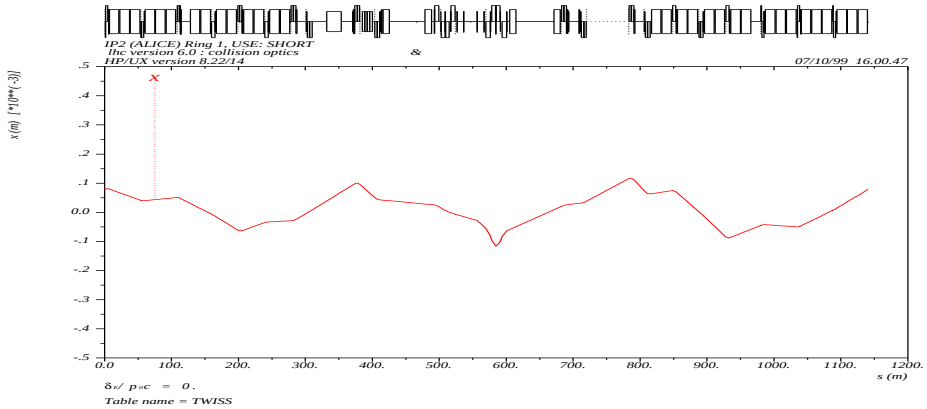

Figure 21: Spectrometer magnet tilted in IP2, not corrected.

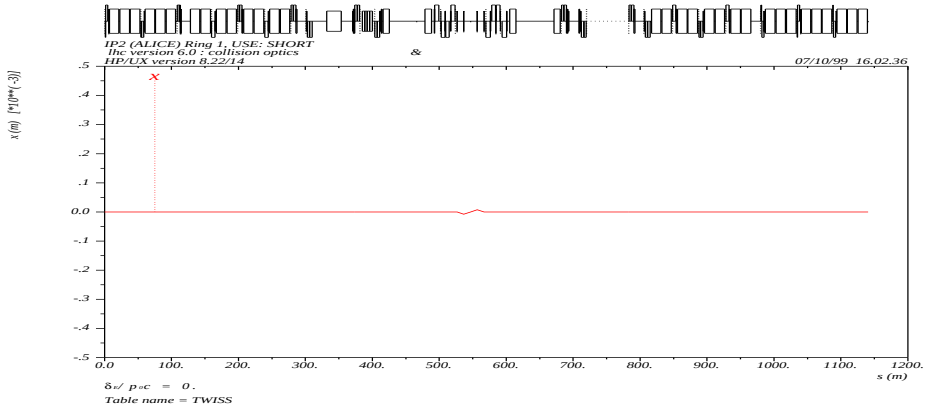

Figure 22: Spectrometer magnet tilted in IP2, corrected by tilting compensator magnets.

[6] O. Brüning; *Optics Solutions in IR8 for Ring-1 and Ring-2 of the LHC Version 6.0*, LHC Project Note 193 (1998).

[7] O. Brüning and J.B. Jeanneret; *Optics Constraints imposed by the injection in IR2 and IR8*, LHC Project Note 141 (1998).

[8] W. Herr; *Effect of PACMAN bunches in the LHC*, LHC Project Report 39 (1996).

[9] J. Poole, F. Zimmermann (eds); *Proceedings of the Workshop on Beam-beam Effects in Large Hadron Colliders*, CERN/SL/99-039 (AP) (1999).

[10] G. von Holtey; Private communication.

[11] J.B. Jeanneret and R. Ostojic; *Geometrical aperture in the LHC Version 5.0*, LHC Project Note 111 (1997).

Appendix A

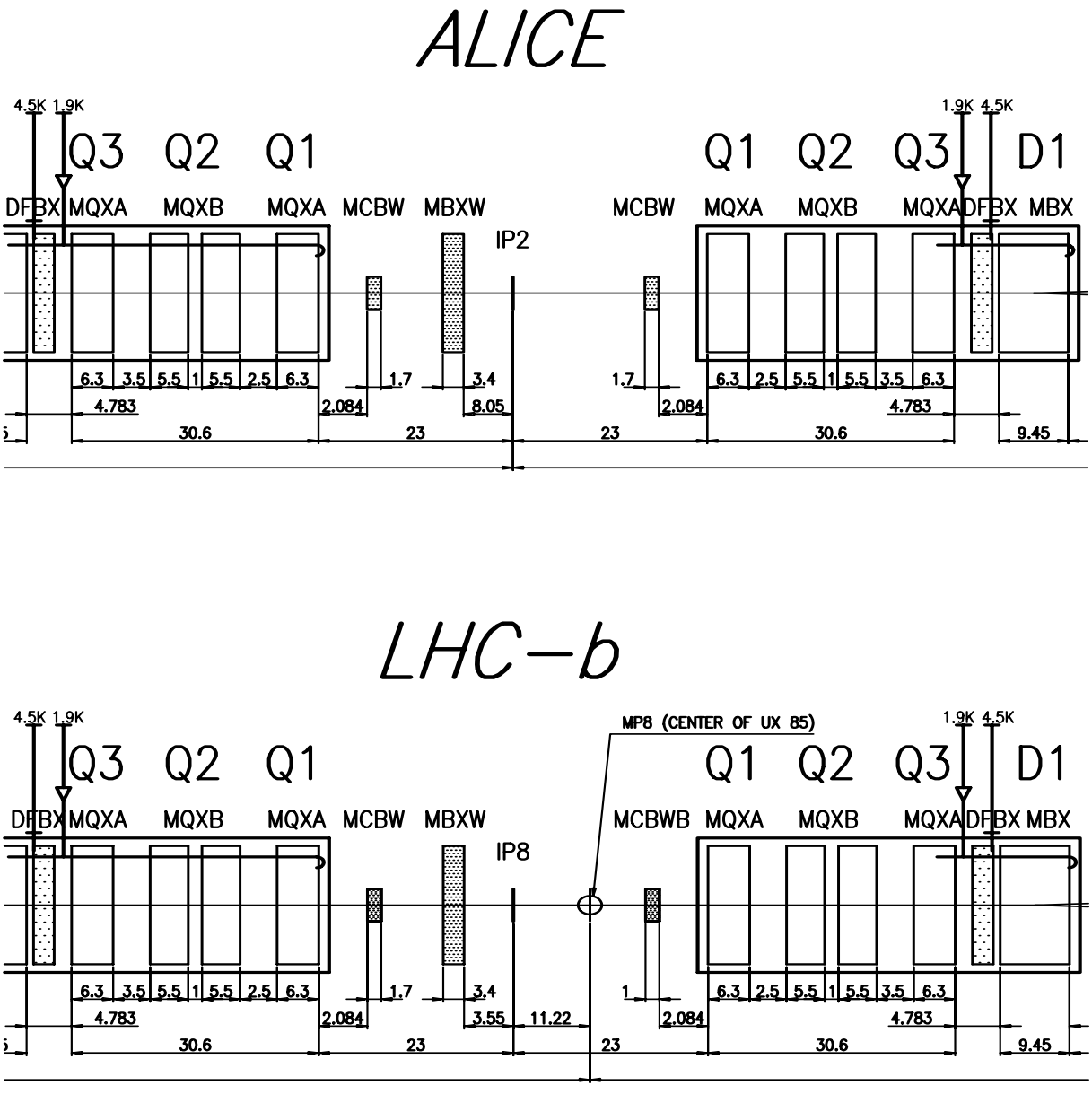

Figure 23: Mechanical layout for spectrometer compensation in IP2 (ALICE) and IP8 (LHCb). The spectrometer dipoles are not included in the figure.

Appendix B

Type	Maximum field (T)	Mag. length (m)	Max. $\int Bdl$ (Tm)	Max. angle at 7 TeV (μrad)
MBXW	1.38	3.43	4.690	$\pm$ 200.0
MCB	3.0	0.84	2.520	$\pm$ 108.0
MCBL	3.0	1.25	3.750	$\pm$ 160.7
MCBY	3.0	0.84	2.520	$\pm$ 108.0
MCBX (h)	3.3	0.50	1.650	$\pm$ 70.7
MCBX (v)	3.3	0.50	1.650	$\pm$ 70.7

Table 5: *Properties of available correction magnets.*

Name	Type	Angle (μrad)	$\int Bdl$ (Tm)
KCV6.L2	MCB	-1.005	0.023
KV1.L2	MCBY	58.34	1.361
KV1.R2	MCBY	9.53	0.222
KV2.R2	MCBY	-49.09	1.145

Table 6: *Required corrector strengths for* $\alpha = \alpha_{ext} + \alpha_{spec} = \pm$ *100* μ*rad in IP2 collision optics at 7 TeV (*β^* *= 10 m, spectrometer ON negative, 3 compensation magnets).*

Name	Type	Angle (μrad)	$\int Bdl$ (Tm)
KCV6.L2	MCB	0.654	0.015
KV1.L2	MCBY	29.02	0.677
KV1.R2	MCBY	16.66	0.389
KV2.R2	MCBY	-31.03	0.724

Table 7: *Required corrector strengths for* $\alpha = \alpha_{ext} + \alpha_{spec} = \pm$ *150* μ*rad in IP2 collision optics at 7 TeV (*β^* *= 10 m, spectrometer ON positive, 3 compensation magnets).*

Name	Type	Angle (μrad)	$\int Bdl$ (Tm)
KCV6.L2	MCB	12.92	0.301
KV1.L2	MCBY	44.14	1.030
KCVQ1.L2	MCBX	-25.0	0.583
KCVQ1.R2	MCBX	25.0	0.583
KV1.R2	MCBY	32.28	0.753
KV2.R2	MCBY	-76.29	1.780

Table 8: *Required corrector strengths for* $\alpha = \alpha_{ext} + \alpha_{spec} = \pm$ *100* μ*rad in IP2 collision optics at 7 TeV (*β^* *= 0.5 m, spectrometer ON negative, 3 compensation magnets).*

Name	Type	Angle (μrad)	$\int Bdl$ (Tm)
KCV6.L2	MCB	4.40	0.103
KV1.L2	MCBY	22.65	0.528
KCVQ1.L2	MCBX	-15.0	0.350
KCVQ1.R2	MCBX	15.0	0.350
KV1.R2	MCBY	11.36	0.265
KV2.R2	MCBY	-33.05	0.771

Table 9: *Required corrector strengths for $\alpha = \alpha_{ext} + \alpha_{spec} = \pm$ 150 μrad in IP2 collision optics at 7 TeV ($\beta^* = 0.5$ m, spectrometer ON positive, 3 compensation magnets).*

Name	Type	Angle (μrad)	$\int Bdl$ (Tm)
KCV6.L2	MCB	-0.295	0.0004
KV1.L2	MCBY	73.385	0.1108
KV1.R2	MCBY	26.648	0.0400
KV2.R2	MCBY	-71.948	0.1079

Table 10: *Required corrector strengths for $\pm$ 210 μrad in IP2 at injection ($\beta^* = 10$ m, spectrometer OFF, no bump at MKI).*

Name	Type	Angle (μrad)	$\int Bdl$ (Tm)
KCV5A.L2	MCB	794.506	1.192
KV1.L2	MCBY	235.825	0.354
KV2.L2	MCBY	-1228.44	1.843

Table 11: *Required corrector strengths for bump of 2.7 mm at MKI in ring 1.*

Name	Type	Angle (μrad)	$\int Bdl$ (Tm)
KH1.L8	MCBY	39.61	0.924
KH1.R8	MCBY	-34.04	0.794
KCHQ1.L8	MCBX	-14.0	0.327
KCHQ1.R8	MCBX	14.0	0.327
KCH6.R8	MCB	9.85	0.230
KCH7.L8	MCB	-3.89	0.091

Table 12: *Required corrector strengths for $\alpha_{ext} = \pm$ 100 μrad in IP8 collision optics at 7 TeV ($\beta^* = 10$ m).*

Name	Type	Angle (μrad)	$\int Bdl$ (Tm)
KH1.L8	MCBY	24.26	0.566
KH1.R8	MCBY	-29.44	0.687
KCHQ1.L8	MCBX	-14.0	0.327
KCHQ1.R8	MCBX	14.0	0.327
KCH6.R8	MCB	-20.37	0.475
KCH7.L8	MCB	14.68	0.343

Table 13: *Required corrector strengths for $\alpha_{ext} = \pm$ 150 μrad in IP8 collision optics at 7 TeV ($\beta^* = 1$ m).*

Name	Type	Angle (μrad)	$\int Bdl$ (Tm)
KH1.L2	MCBY	26.18	0.611
KH1.R2	MCBY	13.02	0.304
KCHQ1.L2	MCBX	30.0	0.700
KCHQ1.R2	MCBX	30.0	0.700
KH2.L2	MCBY	-4.45	0.104
KCH6.R2	MCB	0.39	0.009

Table 14: *Required corrector strengths for ± 1 mm parallel bump in IP2 collision optics at 7 TeV ($\beta^* = 10$ m).*

Name	Type	Angle (μrad)	$\int Bdl$ (Tm)
KH1.L2	MCBY	4.06	0.095
KH1.R2	MCBY	1.46	0.034
KCHQ1.L2	MCBX	5.0	0.117
KCHQ1.R2	MCBX	5.0	0.117
KH2.L2	MCBY	-0.69	0.016
KCH6.R2	MCB	0.77	0.018

Table 15: *Required corrector strengths for ± 0.2 mm parallel bump in IP2 collision optics at 7 TeV ($\beta^* = 0.5$ m).*

Name	Type	Angle (μrad)	$\int Bdl$ (Tm)
KV1.L8	MCBY	12.52	0.292
KV1.R8	MCBY	25.21	0.586
KCVQ1.L8	MCBX	30.0	0.700
KCVQ1.R8	MCBX	30.0	0.700
KCV5.R8	MCB	-4.42	0.103
KCV6.L8	MCB	0.44	0.010

Table 16: *Required corrector strengths for ± 1 mm parallel bump in IP8 collision optics at 7 TeV (β^* = 10 m).*

Name	Type	Angle (μrad)	$\int Bdl$ (Tm)
KV1.L8	MCBY	9.00	0.210
KV1.R8	MCBY	22.18	0.518
KCVQ1.L8	MCBX	24.0	0.560
KCVQ1.R8	MCBX	24.0	0.560
KCV5.R8	MCB	-4.53	0.106
KCV6.L8	MCB	2.61	0.061

Table 17: *Required corrector strengths for ± 1 mm parallel bump in IP8 collision optics at 7 TeV (β^* = 1 m).*